Received: 1 March 2019 | Revised: 24 May 2019 | Accepted: 28 May 2019

DOI: 10.1002/dep2.78

ORIGINAL RESEARCH ARTICLE

The Depositional Record Open Access
A journal of the International Association of Sedimentologists
WILEY

Supercritical flows overspilling from bypass-dominated submarine channels and the development of overbank bedforms

Adam McArthur[1] | **Ian Kane**[2] | **Guilherme Bozetti**[3] | **Larissa Hansen**[1] | **Benjamin C. Kneller**[3]

[1]School of Earth and Environment, University of Leeds, Leeds, UK

[2]School of Earth, Atmospheric and Environmental Sciences, Manchester, UK

[3]Department of Geology and Petroleum Geology, University of Aberdeen, Aberdeen, UK

Correspondence
Adam McArthur, School of Earth and Environment, University of Leeds, Leeds, UK.
Email: a.mcarthur@leeds.ac.uk

Present address
Guilherme Bozetti, Department of Ocean Sciences and Engineering, Southern University of Science and Technology, Shenzhen, China

Funding information
BP; AkerBP; Equinor; Petrochina

Abstract

Overbank deposits of submarine channels are typically thin-bedded, fine-grained and predominantly characterized by a series of sedimentary structures interpreted to record a relatively simple history of waning flow. Here, a new type of bedform indicative of Froude-supercritical flow is reported from successions of thin-bedded turbidites interpreted as channel overbank deposits in the Upper Cretaceous Rosario Formation, Baja California, Mexico. A link is demonstrated between the development of overbank deposits in the form of depositional terraces or internal levees and contemporaneously active sediment transport, bypass and deposition of coarser-grained material in a channel. The overbank bedforms overlie an erosion surface and contain a suite of sedimentary structures indicative of initially Froude-supercritical flow conditions and a progressive waning of flow strength. In some cases, a stacked repetition of facies is interpreted to record a rejuvenation of flow energy. The characteristic sedimentary sequence observed is as follows: (a) long wavelength, low amplitude erosional surface with superimposed scours; (b) antidune backsets; (c) upper stage plane-parallel lamination; (d) subcritical climbing ripples; (e) supercritical climbing ripples; (f) lower stage planar laminated tops; (g) a sharp upper surface. The exact vertical sequence of sedimentary structures encountered varies depending on the point of observation with respect to the bedform crest and distance from the parent channel. The recognition of these distinctive bedforms allows for interpretation of sediment bypass and proximity to a channel thalweg. These bedforms have not hitherto been described and provide a further example of the range of flow processes operating in submarine channel–levee systems, which aids depositional environment interpretation in both subsurface and outcrop studies.

KEYWORDS

Baja California, deep-marine, Rosario Formation, slope channels, turbidity currents, Upper Cretaceous

1 | INTRODUCTION

Submarine channels are ubiquitous geomorphological features of Earth's continental slopes and act as important conduits for the transfer of sediment from the shelf to deep ocean basins (Buffington, 1952; Menard, 1955; Komar, 1973; Peakall et al., 2000; Kneller, 2003; Babonneau et al., 2004). Their sedimentary record typically suggests prolonged periods of erosion, bypass and sediment transfer, which may leave an incomplete record within the channel (Stevenson et al., 2015). A more complete record of channel evolution is commonly found in the overbank deposits that flank them (Kane et al., 2007; Kane and Hodgson, 2011; Hansen et al., 2015, 2017). Large-scale, fine-grained bedforms adjacent to submarine channels, occurring on levee flanks or depositional terraces, have been documented from seafloor and seismic datasets around the world (see review by Symons et al., 2016). These have been attributed to formation under Froude-subcritical flow conditions (densimetric Froude number <1, but see Huang et al., 2009) as internal lee waves (Flood, 1988; Kneller and Buckee, 2000; Lewis and Pantin, 2002), or to Froude-supercritical flow (Froude number >1), forming as antidunes (Normark et al., 1980; Wynn et al., 2000; Ercilla et al., 2002) or cyclic-steps (Cartigny et al., 2011; Kostic, 2011; Zhong et al., 2015). Beneath typical seismic resolution, smaller, coarser-grained overbank bedforms attributed to Froude-supercritical flow have been reported from seafloor channel–levee systems (Normark et al., 1983; Wynn et al., 2002; Hughes Clarke, 2016; Hage et al., 2018) but only a few examples are known from outcrop studies (Winn and Dott, 1977; Ito and Saito, 2006; Lang et al., 2017), where high-resolution studies of the preserved sediments are possible.

Here, a new type of sandstone overbank bedform is described from outcrop; these bedforms are interpreted to have developed predominantly under Froude-supercritical flow conditions. Recognition of these bedforms in outcrop plugs a gap in the knowledge of how overbank features, occasionally observed on the seafloor (Normark et al., 2002), are formed and preserved. Identification of these bedforms in the rock record is significant as they are important indicators of proximity to a bypassing channel. Indicators of bypass in deep-marine strata include: the presence of erosional surfaces; the presence of a lag, that is, some relict sediment that did not 'bypass'; the reworking of pre-existing deposits; or simply a surface with neither deposition nor erosion (Stevenson et al., 2013, 2015). Whether bypass involves erosion depends on the shear strength of the flow versus the nature of the bed (either the shear strength of a cohesive bed or the grain size of non-cohesive materials), such that not all bypassing flows are associated with erosion (Kneller, 1995). Where bypass surfaces are erosional, the record of erosion may be represented either by a surface that truncates beds or laminae, or, more cryptically, a bedding-parallel surface (Stevenson et al., 2013). Within the deep-marine channel-belts that contain slope channels, significant bypass occurs within the channels themselves and the resultant channel-fills can be a partial record of that; however, the stratigraphic record of bypass within a channel is generally more complete within the overbank areas adjacent to channels, typically consisting of thinner bedded and finer grained successions (Piper and Normark, 1983; Kane et al., 2007; Hansen et al., 2015).

Indications of bypass may therefore be cryptic but are crucial in the interpretation of ancient sedimentary sequences, in particular determining the position of a particular succession in both depositional dip and strike profiles of the system. This is perhaps most relevant in the study of deep-water sedimentary successions during hydrocarbon exploration and field development, for example, in predicting the likelihood of sediment bypass to areas down the depositional dip profile. Here, bedforms developed within overbank successions that can be tied to a contemporaneously active channel are investigated with the aim of better understanding the range of flow processes active in submarine channel–levee systems. Specific objectives of this study are:

- Characterize a heterolithic succession of sediments adjacent to a documented slope channel system.
- Utilize outcrop observations to develop insights into the physical behaviour of flows that were overspilling from an active channel.
- Develop a conceptual model for the observed relationships between channel-fill and overbank bedforms that demonstrate deposition from flows during Froude-supercritical flow conditions.
- Consider implications for the interpretation of overbank bedforms resulting from Froude-supercritical flow in both subsurface and outcrop studies.

The study focuses on an individual channel complex within the San Fernando channel–levee system of the Upper Cretaceous Rosario Formation, Baja California, Mexico (Figure 1).

2 | GEOLOGICAL SETTING OF THE ROSARIO FORMATION

The Upper Cretaceous to Palaeocene Rosario Formation crops out discontinuously along the Pacific coastal margin of southern California and Baja California (Beal, 1948; Gastil et al., 1975) (Figure 1). The Rosario Formation was deposited in the Peninsular Ranges fore-arc and consists of shallow-marine and deep-marine sediments predominantly sourced from volcanic and plutonic rocks of the Upper Jurassic to Lower Cretaceous arc complex to the east, but was also derived from sedimentary and metasedimentary rocks of the

fore-arc (Gastil et al., 1975; Morris and Busby-Spera, 1990; Busby et al., 1998).

The features described here belong to a slope channel–levee system, termed the San Fernando channel–levee system, which crops out in and around Arroyo San Fernando (Morris and Busby-Spera, 1990; Li et al., 2018; Kneller et al., 2019). The slope channel system consists of a *c.* 500 m thick, 7 km wide succession of conglomerates, sandstones, siltstones and mudstones, bounded to the north-west by a roughly 2.5 km wide belt of inter-bedded sandstones and mudstones interpreted by Morris and Busby-Spera (1990), Dykstra and Kneller (2007) and Kane et al. (2007) as an external levee (sensu Kane and Hodgson, 2011). This slope channel system initially onlaps mudstones to the south-east (Figure 2; Dykstra and Kneller, 2007), indicating that the system was oblique to the regional slope, which is thought to represent an underlying structural control (Dykstra and Kneller, 2007; Kane et al., 2009).

At least four major episodes of coarse-grained input and channel development occurred (Figure 2, channel complex sets A–D, following the terminology of Sprague et al., 2002), each with multiple channel complexes and associated overbank deposits (Figure 2; Kane et al., 2009, 2010a; Kane and Hodgson, 2011; Callow et al., 2013; McArthur et al., 2016; Hansen et al., 2017; Li et al., 2018). These coarse-grained intervals are separated by mudstone-dominated thin-bedded turbidites, debrites and hemipelagites representative of background sediment deposition across the channel-belt (Li et al., 2018). The focus of this study is a single channel complex (sensu Sprague et al., 2002), which occurs within Channel Complex Set B of Li et al. (2018) and is informally termed the 'S-Channel' (Figure 3).

3 | METHODS

Field observations were recorded predominantly by logging sections of the outcrop and tracing key stratigraphic surfaces, where possible on foot, but also with the use of photomosaics. Numerous valleys carved into the outcrops offer three-dimensional exposure of both the channel-fill and the associated thin-bedded overbank successions below, lateral to, and above

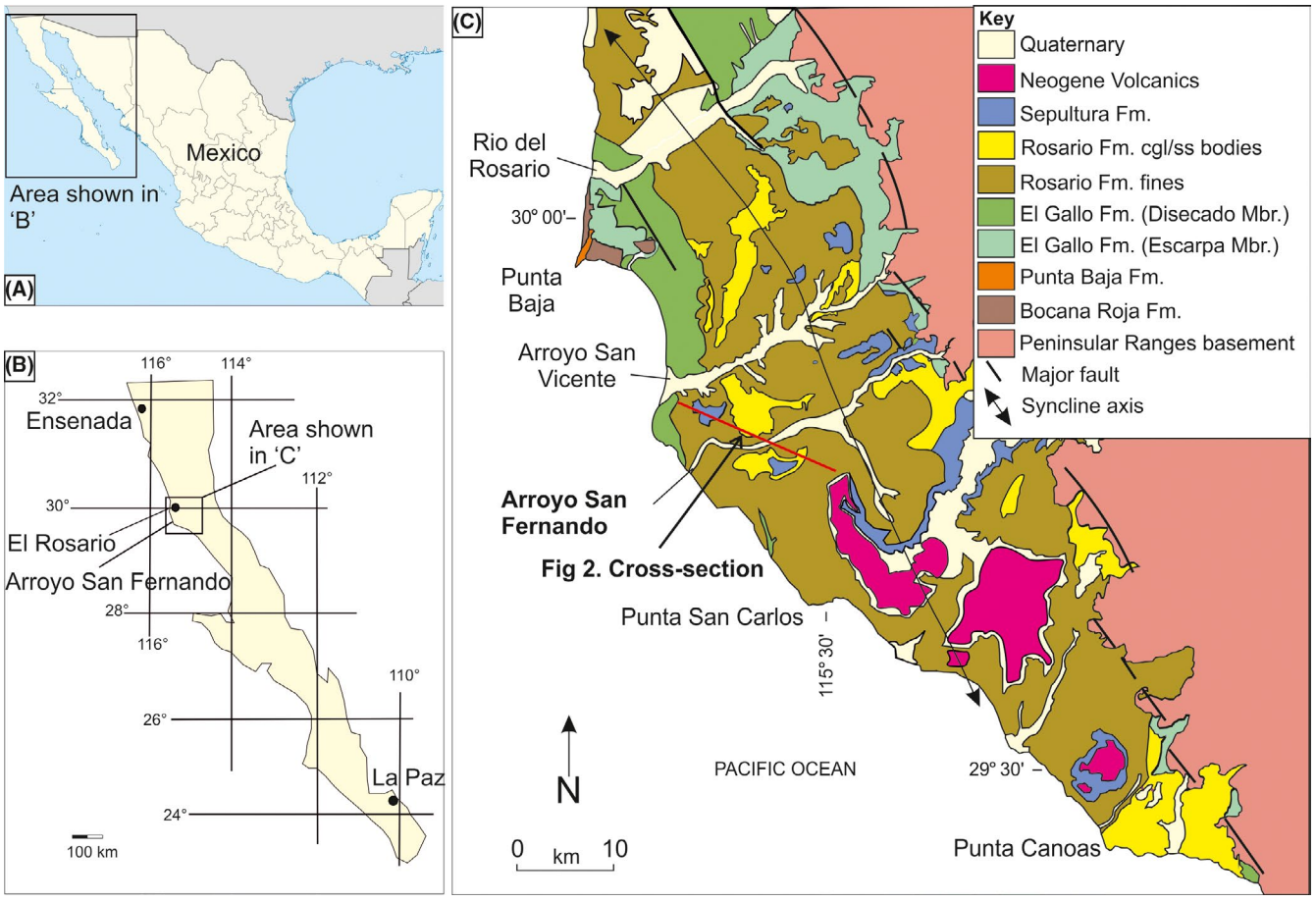

FIGURE 1 (A) The position of Baja California, Mexico; (B) Baja California peninsula and El Rosario, the closest town to Arroyo San Fernando; (C) simplified geological map and stratigraphy of the region surrounding Arroyo San Fernando, modified from Morris and Busby-Spera (1990), Alexadri-Rionda et al. (2008), Dykstra and Kneller (2009) and Kane et al. (2009). The study area is highlighted by the cross-section of Figure 2

the coarse-grained channel-fill. A dextral, post-depositional strike-slip fault with approximately 30 m of displacement duplicates the studied channel margin offering two perspectives through the same cut (Figures 4 and 5). Digital mapping of the channel and surrounding outcrops was undertaken using GPS. Bed thicknesses, clast imbrication, ripple foreset orientation, grain and gravel clast sizes were recorded (Figure 5).

4 | RESULTS

4.1 | Facies Associations

The facies of the Rosario Formation in the area of Arroyo San Fernando have been described by previous authors (Morris and Busby-Spera, 1988, 1990; Dykstra and Kneller,

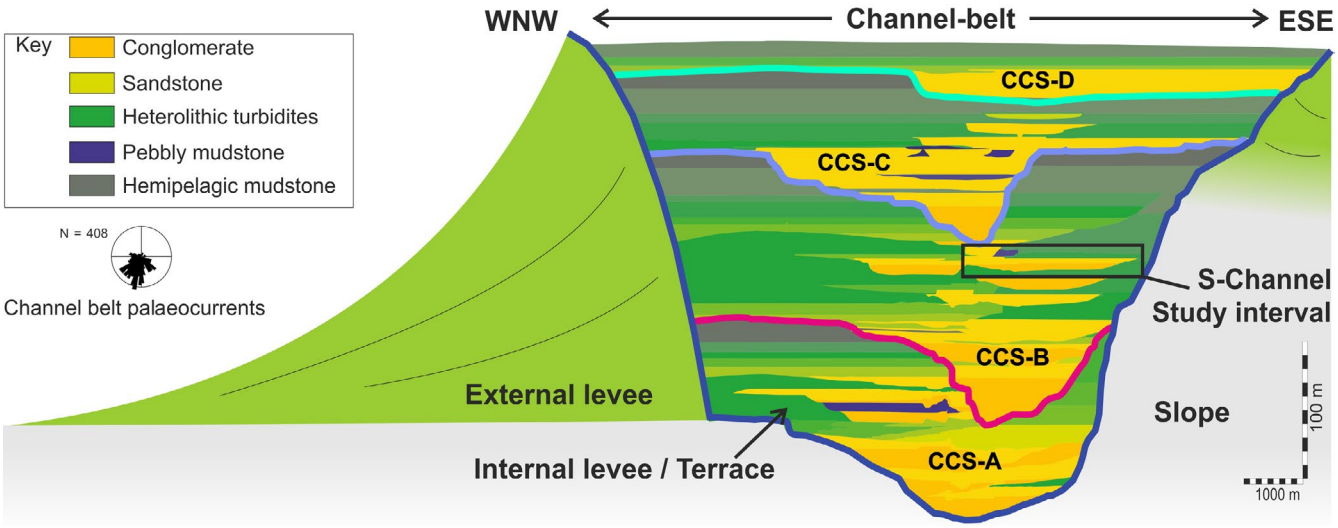

FIGURE 2 Simplified WNW-ESE cross-section of the San Fernando channel–levee system, modified from Morris and Busby-Spera (1990), Hansen et al. (2017) and Li et al. (2018). CCS = channel complex set. Overall palaeoflow of channel-belt towards reader, with palaeocurrent data from Dykstra and Kneller (2007)

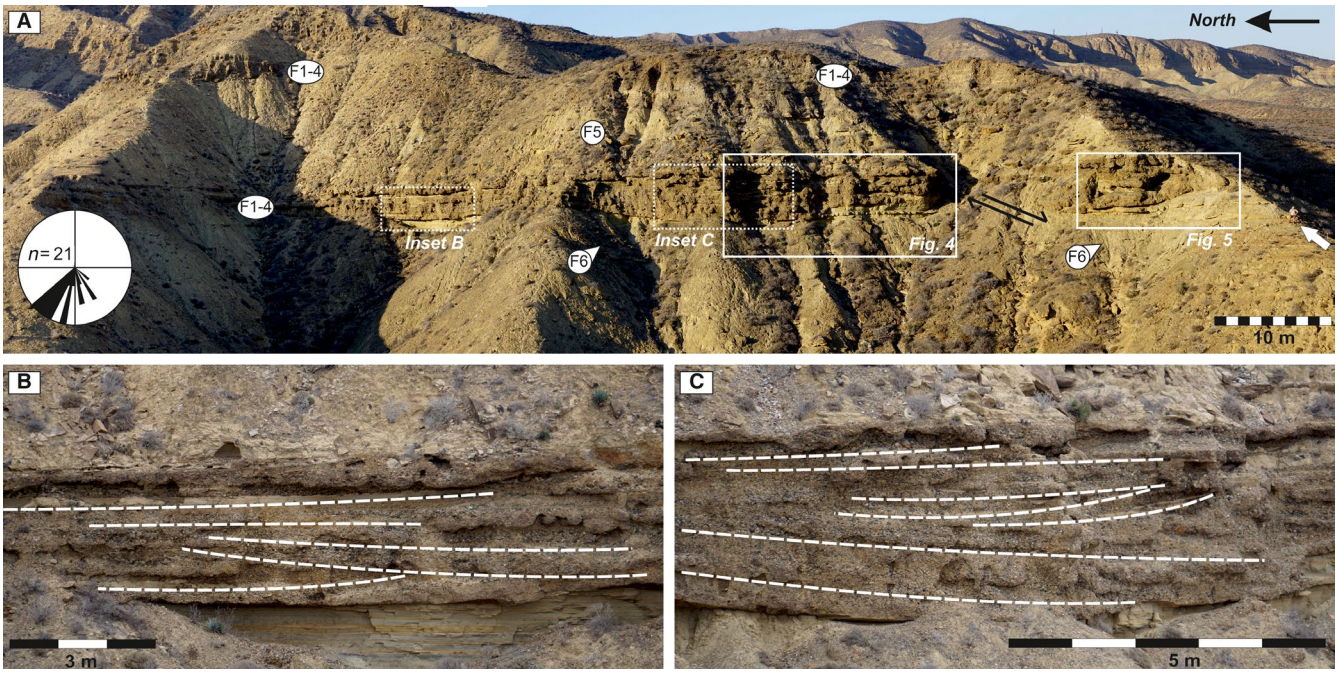

FIGURE 3 Overview of the 'S-Channel' showing the coarse-grained part of the channel-fill standing proud of the hillside. (A) An upper, sand-rich part is less clearly exposed. A strike-slip fault to the south of the outcrop repeats the margin. Note the person for scale standing on the overbank deposits (arrowed, on the far right). (B) and (C) are insets, with dashed lines to illustrate some of the lateral-accretion surfaces within the channel-fill. The section is oriented north-south with palaeoflow towards the southwest, as illustrated by palaeocurrent data from Li et al. (2018) supplementing field observations

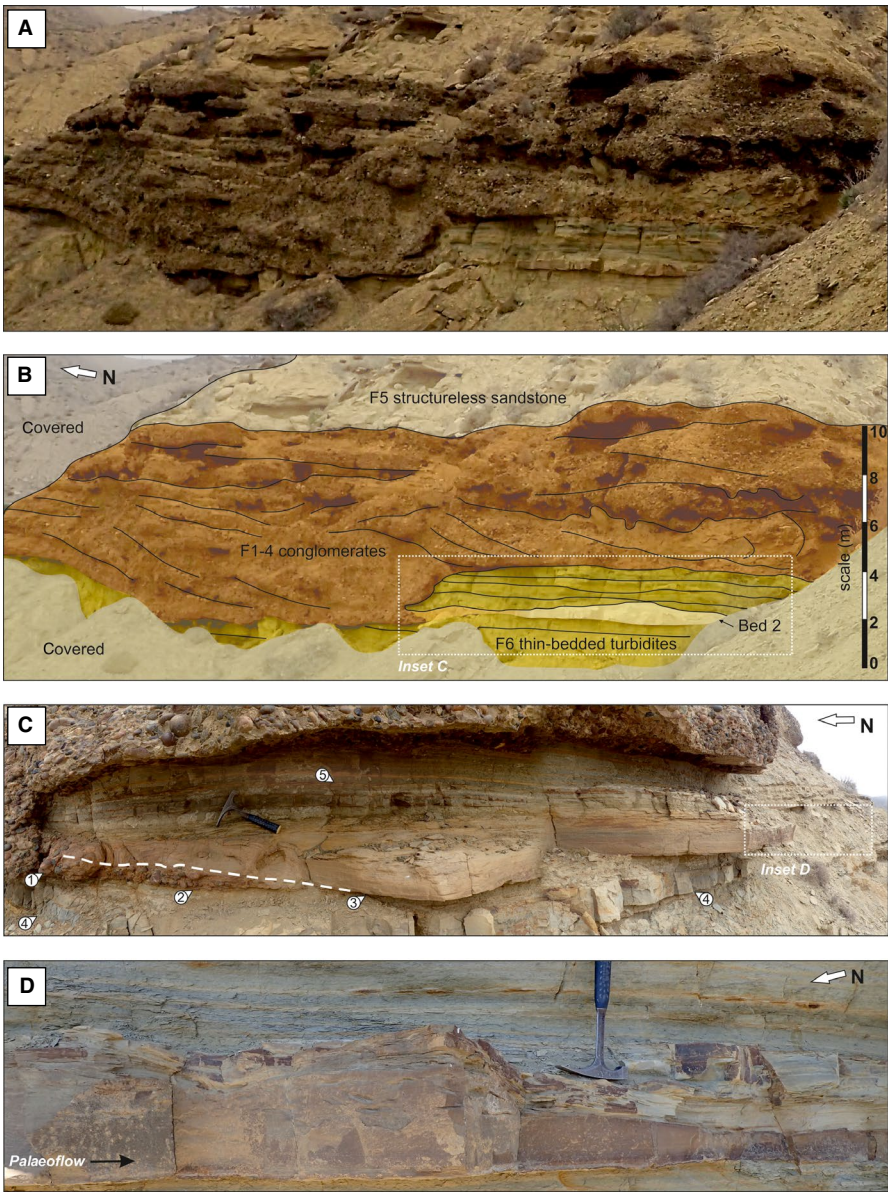

FIGURE 4 Scales of transition from conglomerates to thin-bedded strata from (A) SE margin of the S-Channel. (B) Line drawing interpretation of the margin, demonstrating the relationship of the channel-fill conglomerates to overbank strata, with bed 2 showing a transition from intra-channel conglomerate to thin-bedded facies. (C) Close-up photograph of conglomerate wing (1) transitioning to (2) gravel bedforms (below dashed line) at the base of the sandstone (3), overlying a marl bed (4) and itself overlain by thin-bedded turbidites showing climbing ripples (5); details on the bedforms are presented in subsequent figures. (D) Lateral view of bed 2 transition from medium-bedded sandstone into a thin-bed. Note, hammer for scale is 28 cm long

2007; Kane et al., 2007; Kane et al., 2009; Callow et al., 2013; McArthur et al., 2016; Hansen et al., 2017; Li et al., 2018). Based on the work of these authors and observations made as part of this study, a sixfold facies scheme is employed here (F1–F6) which is summarized in Table 1. For the purpose of this study of the S-Channel, the facies are grouped into two distinctive facies associations, FA1 = F1–5 and FA2 = F6.

4.1.1 | FA1: Channel-fill

Observations

A wide range of facies comprise this association, including F1–F5 (Table 1). The facies association is dominated by F1 (clast supported conglomerates), which occurs as horizontally bedded units at the base of coarse-grained intervals, but mostly as inclined strata inter-bedded with subordinate F2–F5 conglomerates and sandstones (Figure 3). Inclined surfaces within the coarse-grained intervals dip at around 10° (Figure 3B,3). Palaeocurrents from clast orientations (dominantly A-axis inclined/B-transverse, with lesser A-transverse/B-inclined) are oblique to perpendicular to the dip of the inclined surfaces and show a general direction to the SW (Figure 5). Matrix-rich facies (F2 and F3) occur as isolated patches mostly in, but not restricted to, the upper parts of coarse-grained intervals (Figure 4A). This association forms lenses hundreds of metres wide and up to 10 m thick, which show stepped incisions into underlying strata, in this case represented by FA2, by which it is also laterally bound (Figure 6). Despite the complexity of internal erosion surfaces, individual beds may be seen to fine towards their lateral margins. Although the lower portion is dominated by conglomerates of F1–F4, a structureless sandstone (F5) ~4 m thick overlies the conglomeratic portion, giving it a general fining-up trend (Figure 3A).

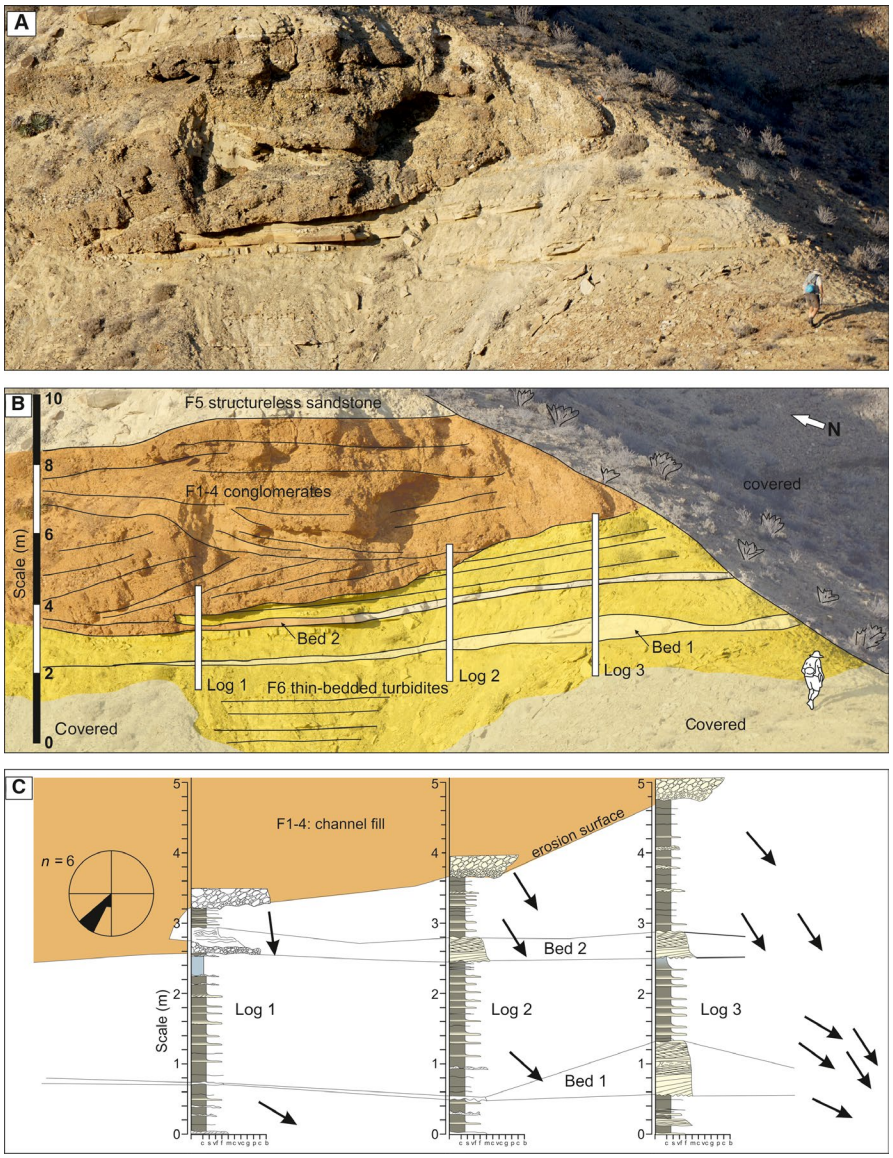

FIGURE 5 (A) Close-up photograph of the fault repeated SE margin of the S-Channel. (B) Line drawing showing the position of the lenticular sandstones illustrated in Figures 6–9. (C) Measured sections through the lenticular beds and channel margin. Note the erosional base of the channel-fill, which truncates the underlying thin-bedded strata. Bed 1 coincides with the channel margin several hundred metres to the northwest (left in the photo). Palaeoflow measured from imbrications within the conglomerates (shown in rose diagram) and individual ripples in the adjacent strata (shown as arrows)

Interpretation

Deposits similar to these have been described from other parts of the Rosario Formation (Dykstra and Kneller, 2009; Kane et al., 2009) and the wider context of this channel complex set has been described by Li et al. (2018). This facies association was ascribed to the late stage fills of coarse-grained slope channels dominated by lateral-accretion, within the wider channel-belt (Li et al., 2018), that is, these are the deposits of parts of flows confined within a channel thalweg (i.e. the deepest part of the channel). The lateral-accretion surfaces have a relatively high aspect ratio (>1:20), steep dip angles (~10°) with palaeoflow approximately parallel to their strike orientation, which implies that these channels were sinuous and the resulting deposits formed by lateral migration, without significant incision or aggradation (Li et al., 2018). That these sinuous channels (maximum preserved width 1,250 m) were able to migrate across a wider channel-belt (~5 km wide) implies availability of significant space for overbank material to accumulate (Kane and Hodgson, 2011; Hansen et al., 2017; Li et al., 2018).

4.1.2 | FA2: Overbank deposits

Observations

The succession immediately adjacent to FA1 is dominated by thinly inter-bedded sandstones and mudstones (F6), and is tens of metres thick in places (Figure 3). Given the less resistant nature of these finer grained deposits compared with the conglomeratic channel-fills, their full lateral extent is not revealed due to weathering, erosion and cover. Here, they are traceable up to 20 m away from the channel-fill (Figure 3); elsewhere in the Rosario Formation accumulations of thin-bedded material hundreds of metres thick and kilometres

TABLE 1 Principal facies types of the Rosario Formation examined in the present study

	Facies 1: Clast-supported conglomerate Description: Closed framework, orthoconglomeratic, polymict, with sub- to well-rounded pebble to boulders. Clasts are dominantly extra-formational with lesser intra-formational mudstone clasts. Grain fabric is anisotropic with common A-axis parallel and inclined fabrics. Beds may be normally, non- or inverse graded. The matrix is very fine to fine sand. Turitella and Ostrea fragments are common. Interpretation: The grain fabric and low clay-silt content indicate tractional transport as bedload (e.g. Walker, 1975, 1978). A-parallel fabrics are indicative of intense laminar shear of high-concentration flows (Rees, 1968, 1983; Allen, 1982; Postma et al., 1988); the A-transverse fabrics in these relatively well-sorted deposits are suggestive of rolling beneath an overriding turbidity current (Walker, 1975, 1978). It may be possible by winnowing and tractional reworking to produce clast-supported conglomerates from matrix-rich or matrix-supported deposits (Collinson and Thompson, 1982), but the strong fabric in this facies precludes that interpretation.
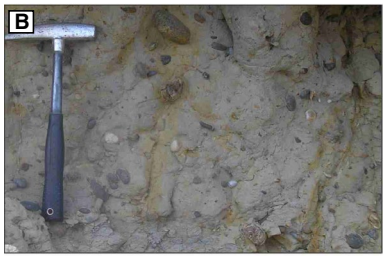	Facies 2: Matrix-supported conglomerate Description: Clasts range from monomict to polymict. Monomict examples may be texturally mature (well-sorted pebbles), relatively immature (well-rounded shale clasts, 10–300 mm in length), to very immature (angular shale/thin-bedded clasts 10 to >1,000 mm in length). Although monogenic types are common, most are polygenic and also include shell and bone fragments. Clasts are dominantly extra-formational with lesser intra-formational mudstone clasts. Clasts typically show random orientations or may be horizontal (parallel to bedding). The matrix is usually composed of mud and silt although some are slightly coarser (very fine to fine sand) or may contain sandy pockets or streaks. Interpretation: These are attributed to cohesive sediment gravity flows (Winn and Dott, 1979; Lowe, 1982; Morris and Busby Spera, 1988, 1990). However, there is a continuum between facies ascribed to traction/bedload transport and deposition and those ascribed to debris flow transport and deposition. Pebbly mudstones suggest laminar transport in which particles were supported by the plastic strength of the flow (e.g. Crowell, 1957).
	Facies 3. Matrix-rich conglomerate Description: Matrix-rich conglomerates are generally less sorted and lack the organized fabric of those with minimal matrix. Two endmembers of this facies are observed: clast-rich conglomerates with a sandy matrix, and clast-poor conglomerates with a muddy-sandy matrix. In general, the higher the mud content within the matrix, the less well-pronounced grading may be, with muddier sediments exhibiting little or no grading. Conglomerates include both extra- and intra-formational clast-dominated examples. Interpretation: The lack of strongly organized clast fabrics indicates limited bedload transport immediately prior to deposition, with little or no tractional reworking of clasts; these conglomerates were probably deposited and covered relatively quickly. Clast-supported conglomerates with a high matrix content suggest transport by flows which were transitional between turbulent and laminar (cohesionless); conglomerates which have a higher matrix content, which tends to be clay rich, may be ascribed to flows where cohesion was increasingly important. Angular rafts of heterolithic material suggest that these deposits are sometimes relatively immature; flows may have evolved downslope into fully turbulent flows within which rafts of sediment would rapidly be broken up.
	Facies 4: Inter-bedded sandstones and conglomerates Description: Dominantly clast-supported conglomerates as described above (Facies 1), inter-bedded with tractional sandstones. Conglomerates are thin- to thick bedded and variably graded. Boundaries between congomerates and sandstones are generally sharp. Sandstones are very fine- to fine-grained, sometimes with intervals of sub-angular to angular, granular extra-formational clasts. Sandstones are characterized by plane-parallel and low-angle cross lamination. Trains of granules and clasts can occur along lamination surfaces, with some larger clasts appearing to be isolated within sandstones Interpretation: These deposits are interpreted as representing tractional transport within polydisperse flows; clasts are transported along the bed by powerful sand-bearing turbulent flows, whilst sand is deposited from suspension and reworked along the bed. Establishing single event beds or genetic links between conglomerate-sand couplets is generally not possible.

(Continues)

TABLE 1 (Continued)

Facies 5: Structureless/tractional – dewatered sandstones

Description: These are up to 5 m thick and tend to occur overlying conglomerate bodies. They are typically very fine- to fine-grained and lack depositional structure, including grading. However, dewatering structures, such as pipes and dishes, are evident in some sections along with remnant/deformed lamination. Bed bases generally appear non-erosional; however, erosional remnant blocks are occasionally found at the bases of some sandstones. Small, scattered mud flakes (1–3 mm) are common.

Interpretation: Deposition from decelerating and strongly depositional flows (Kneller and Branney, 1995). Alternatively, flows may have been relatively steady but strongly depositional due to very high sediment concentrations (Leclair and Arnott, 2005; Lowe, 1988). Erosional remnants suggest that flows may have been capable of significant erosion, or were deposited on top of bypass surfaces of earlier flows. Dewatering structures suggest that original tractional structures may have been removed (e.g. Lowe, 1975), 'autokinetic' pore-pressure fluctuations associated with overriding gravelly flows may be important in these environments (Røe and Hermansen, 2006).

Facies 6. Inter-bedded thin sandstones and mudstones

Description: Laterally extensive thin-bedded sandstones and mudstones. Sandstones are very-fine to fine grained with sharp, occasionally erosional bases. Subcritical climbing and non-climbing current ripple cross lamination are the dominant sedimentary structures (~80% of beds), planar lamination is less common (<10%). Finer divisions consist of siltstone to mudstone, commonly foraminifera-rich. Palaeocurrents may be complex. Lenticular sandstones, which form the basis of this paper, also occur (indicated with an arrow in the photo).

Interpretation: These thin beds are interpreted as low-density turbidites overspilled from an adjacent thalweg, with each sand-mud couplet comprising one episode of overspill. Their character suggests that they are the product of reflected and deflected, unsteady flows, hinting at topographic influence on flows, both within and outside the channel. This facies strongly resembles the internal levee facies of Kane and Hodgson (2011), although a wedge-shaped geometry cannot be demonstrated here. The lenticular sandstones arrowed form the discussion of this manuscript.

wide are present (Kane et al., 2007; Kane and Hodgson, 2011; Hansen et al., 2017). The general palaeocurrent direction is SE, being 45–90° less than those of FA1 (Figure 5). Trace fossils, generally absent within FA1 are widespread in FA2, including *Phycosiphon*, *Scolicia*, *Planolites* and *Ophiomorpha*. Foraminifera, including agglutinated forms such as *Bathysiphon* sp., are common in the mudstones. Within these thinner bedded successions, erosional based, lenticular sandstones, a few to 75 cm thick occur, which are described in detail below (Figure 4). At the bases of channel-fills, there are clear lateral transitions between FA2 and FA1 (Figure 6A), whereas higher in the succession, the incisional contact makes it impossible to relate any one thin-bed to intra-channel deposits (Figure 5).

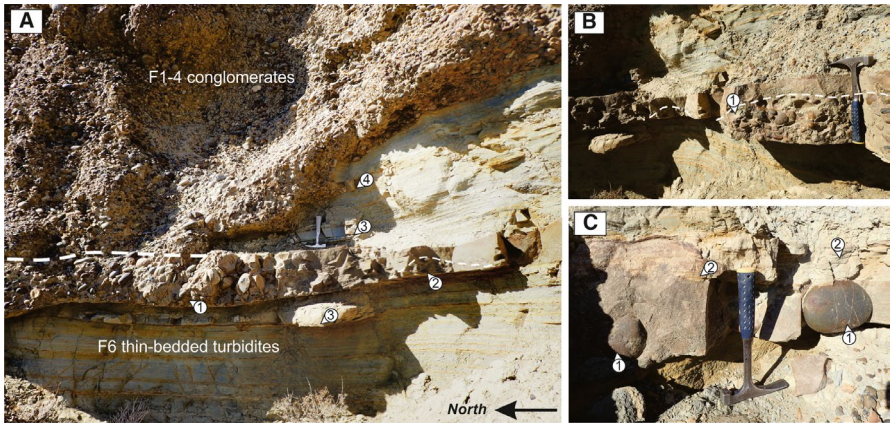

FIGURE 6 Margin of the S-Channel. (A) Conglomerate at the base of the channel-fill (below dashed line in conglomerate body) extending into a sandstone bed within the overbank succession (1); (2) gravel at the base of the sandstone; (3) marly, bioturbated concretion within the overbank succession; (4) smaller conglomerate 'wing' extending into a thicker sandstone in the overbank succession. Note hammer in centre of picture for scale. (B) Gravel lens in the sandstone bed, it is thickest beside the hammer handle and pinches towards and away from the channel (1). (C) Isolated large cobbles sat on the basal erosion surface of the thick sandstone bed (1) overlain directly by laminated sandstone (2)

Interpretation

The thin-beds are overbank sediments that were deposited by the low-density upper portions of turbidity currents, whose higher density basal layer was confined within the channel axis (FA1), that is, these deposits represent the relatively unconfined portion of flows overspilling from channels (Peakall et al., 2000). Proximity to the channel thalweg, as well as larger scale topography confining the entire channel-belt, is suggested by complicated palaeocurrent patterns, the presence of erosional structures at bed bases and internally within beds, features which are absent from the external levee that bounds this system (Kane et al., 2007; Kane and Hodgson, 2011; Hansen et al., 2015) and in external levees elsewhere (Kane and Hodgson, 2011; Morris et al., 2014). These deposits are therefore interpreted as overbank deposits to a channel within a broader channel-belt (stage II fill of Li et al., 2018, their fig. 14). In this locality, the three-dimensional geometry of these deposits is uncertain. The presence of trace fossils and foraminifera implies time between flows to allow for colonization and that these deposits do not represent intra-channel sediments, which show restricted fossil assemblages (Callow et al., 2013). This thin-bedded succession has been described previously as representing internal levee deposits (Li et al., 2018) or as flat-topped 'depositional terraces', formed due to limited flow expansion space (Hansen et al., 2015, 2017). There is most likely a continuum between the two types of deposits and their differentiation here is challenging since a wedge-shaped (levee) geometry cannot be unambiguously demonstrated. In either case, they are associated with actively migrating channels within a broad channel-belt. The lenticular sandstones that form the focus of this study are interpreted as the product of overbank bedforms and are described in more detail below. Lateral transitions into conglomerate facies are interpreted as indicative of on-axis to off-axis positions within the channel-belt, as described by Kane et al. (2009) from the underlying system, but discussed in more detail with reference to the overbank bedforms below.

4.2 | Lateral facies transitions

4.2.1 | Observations

In some cases, the overbank bedforms or the erosion surfaces they lie on can be traced laterally into coarse-grained channel-fill (FA1) (Figures 4–6). The S-Channel is a conglomerate channel-fill with multiple orientations of lateral-accretion surfaces recording two main migratory phases, first to the south-east and later to the north-west (Li et al., 2018). A basal erosion surface underlying the conglomeratic fill of the channel cuts into a thin-bedded succession (FA2) containing lenticular sandstones (e.g. Bed 2 in Figure 4). Within the conglomerate-filled channel, directly above the erosional cut, a conglomerate variably 20–50 cm thick extends in a wing-like manner from the lowermost part of the channel-fill and passes laterally into a medium-bedded sandstone, which becomes part of the overbank succession (Bed 2 in Figure 5). This sandstone bed has an erosional but generally bedding-concordant base, whilst the top undulates creating a bed that pinches and swells away from the channel margin (Figure 5). The boundary between the conglomerate and the sandstone is gradational, with isolated clasts and accumulations of clasts found at the base of the sandstone (Figure 5). The conglomerate is sandstone matrix-rich compared to that of the overlying conglomerate channel-fill, albeit with some weak imbrication (Figure 6). The conglomerate tapers to the base of the sandstone, with smaller bodies and lenses of imbricated gravel at the base of the sandstone bed isolated from the main conglomerate (Figure 6). The sandstone overlying these facies is massive and possibly dewatered close to the conglomerate but passes laterally into a parallel-laminated, traction-dominated, deposit (Figure 5B). Grain size decreases away from the channel-fill, from very-coarse sandstone, with isolated granular intervals, fining over several metres to medium-grained then fine-grained sandstone (Figure 4C). The sandstone is low-angle planar laminated, the lamination rising away from the conglomerate to form backsets (Figure 5), that is, stratification dipping in the opposite direction to the palaeoflow that is described below.

4.2.2 | Interpretation of facies juxtaposition

There are at least three plausible origins for the development of this facies relationship: (a) lateral injection of the conglomerate at an erosional channel margin into an anomalously thick and unlithified sand within the heterolithic channel-belt; (b) deposition of the sands by part of the same flow that deposited the conglomerate at the base of the channel-fill; (c) the gravel was deposited by one or more flows and the sand by a subsequent flow.

The second or third mechanism(s) are favoured here, for the following reasons: (a) the conglomerate pinches out to the base of the sandstone bed (Figures 4 and 6E). (b) Gravelly lenses occur at the base of the sandstone beds, occasionally with tractional fabrics (Figure 6). (c) Isolated cobbles and pebbles may be found at bedform bases (Figure 6), suggesting that clast deposition may have been more widespread and that these represent winnowed remnants. (d) These large clasts can be overlain by facies within the sandstone bed that retain their sedimentary structures (planar and ripple lamination) (Figure 6C). If the gravels were forcefully injected, it is difficult to envisage the preservation of un-deformed sedimentary structures in the wet sand directly above them. (e) Sedimentary structures within the sandstone beds indicate flow directly away from the conglomerate and record a reduction in flow energy away from the conglomerate within

individual sandstone beds (Figures 4 and 5). (f) Grain size decreases in the sandstones systematically away from the channel-fill (Figure 5). (g) The erosion surface at the base of the bed is concordant from the conglomerate to the sandstone (Figure 5).

Therefore, it is suggested that the overbank bedforms may represent a frontal or lateral splay from the adjacent channel and can be tied directly to the migration and filling of the channel, potentially recording larger bypass events within the channel-belt. Subsequent progradation of the channel results in a vertical facies transition from the frontal/lateral splay deposits (weak confinement) to channel axis deposits (strong confinement).

4.3 | Overbank bedforms

4.3.1 | Observations

Overbank bedforms are uncommon within the thin-bedded succession that is interpreted as overbank to the S-Channel and to other channels within the San Fernando channel-belt. Here, a bedform is defined as a depositional body of sediment which formed a topographic feature on the palaeo-seafloor and is characterized by a stack of sedimentary structures, the order of which varies both laterally and vertically through the preserved bed. As a proportion of beds, they represent <6% of the studied interval, but variably form up to 25% of the thickness of strata adjacent to the channel-fill. The bedforms lie on a basal erosion surface that may pass laterally from the channel-fill (FA1) into the overbank (FA2) as described above or they may form isolated lenticular sandstones (Figure 7). Large cobbles and pebbles may be found in isolation at bed bases nearest to the channel-fill (Figure 6) and the overall grain size diminishes in the direction of palaeoflow (Figure 5). Beyond the downstream termination of a sandstone, a continuous erosion surface is observed that may have complex surface undulations with rare loading structures (Figures 7 and 8). Where sand was not deposited (or preserved) above the erosion surface, the surface may be overlain by siltstone and might easily be overlooked in a succession of thin-bedded turbidites (Figure 8). Small-scours along the erosion surface may be filled with slightly coarser sandstone, lacking the finer tail found in other overbank thin-bedded turbidites (Figure 8). These small-scours occasionally

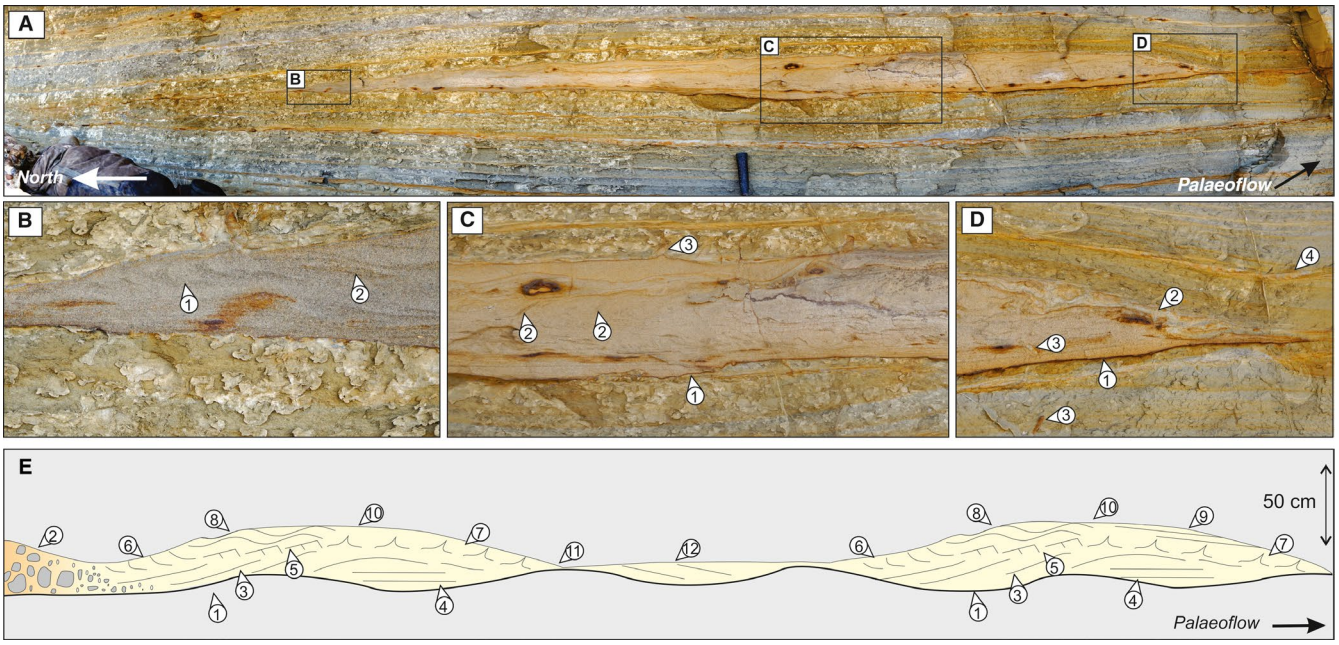

FIGURE 7 Lenticular sandstone occurring beneath the S-Channel. (A) Overview panorama photograph showing the position of inset illustrations. Palaeoflow indicators illustrate approximately left to right sediment transport (SE). Note the hammer handle in the centre for scale. (B) Upstream end of the feature, note the overturned ripple foresets, indicating high rates of shear by an overriding flow (1) and the undisturbed foresets to the right (2). (C) (1) Irregular basal cut through the underlying thinly inter-bedded heterolithic strata. Note the complexity of the erosional cut suggesting that the bed had some strength; (2) internal flame structures; (3) overturned ripple foresets. (D) (1) Erosional base; (2) dewatering structures and soft-sediment deformation at the downstream end of the structure; (3) Ophiomorpha sp. burrow; (4) thickening of overlying muddy sediments, healing the topography of the bedform. (E) Schematic sketch of overbank bedforms to illustrate the key vertical and lateral features (1) irregular basal erosion surface; (2) gravel at the base of the bedform adjacent to the parent channel-fill; (3) sharp-based backsets; (4) low angle/planar lamination; (5) subcritical climbing ripples; (6) overturned ripple foresets; (7) dewatering structures; (8) supercritical climbing ripples; (9) sinusoidal to lower stage planar lamination; (10) sharp top overlain by siltstone; (11) pinch of bedform with continuation of erosional surface; (12) scour fill associated with erosional surface

show loading and a minor degree of injection into adjacent strata, resulting in scours with irregular forms (Figure 8B).

The bedforms overlie these erosion surfaces (Figure 9). They range from a few metres, up to at least 10 m in length, with thicknesses up to 75 cm (Figure 5). The overlying sedimentary structures exhibited by the bedforms show variability in their vertical sequence, but there is a common motif (Figure 7); a typical bedform has the following vertical facies stacking, from the base: (a) planar backsets representing antidune upper stage flow conditions; these can be nearly horizontal to quite steep (10°); (b) upper stage plane-parallel lamination; (c) subcritically climbing ripples (n.b. here subcritical and supercritical refers to the angle of climb, not the flow conditions); (d) supercritically climbing ripples; (e) sinusoidal to lower stage planar lamination; (f) a sharp top surface (Figure 9). Occasionally, lamina is seen to be truncated at the bed top, whilst in others, the bed top is disrupted by small injections and burrows (Figure 7D). The sandstone beds pinch and swell to form prominent bedforms, which may completely terminate above the continual erosion surface (Figures 5 and 9). The wavelength of the pinching and swelling varies, being in the range of several metres. The sandstones are typically overlain by siltstone. Repeated facies stacks in individual bedforms are observed, for example, in the thickest part of Bed 1 (Figure 5). In places, the lower part of the typical facies stack is missing, with the bedform commencing with planar lamination or climbing ripples (e.g. Figure 7B). The central part and downstream end of the sandstone can be dewatered and have undergone soft-sediment deformation (Figure 7D). Within the thin-bedded succession above and below these bedforms, trains of starved and subcritical climbing ripples also commonly overlie minor erosion surfaces (Figure 10). The abundance of bedforms reduces vertically, being most abundant above the erosion surface that can be traced laterally into the channel-fill.

4.3.2 | Interpretation of overbank bedforms

The lateral transitions seen at the base of the channel-fill (FA1) into the overbank (FA2) imply that these bedforms are most common immediately adjacent to the channel-fill and the fact they have not been observed elsewhere in the wider overbank or external levee of San Fernando implies that they are restricted to tens of metres adjacent to individual channels. That bedforms are most prevalent lower in the described section likely occurs due to the parent channel building levee relief, such that the overspill comprises progressively higher parts of the flow, hence slower moving and less concentrated parts of the flow. Therefore, the likelihood of Froude-supercritical conditions being met reduces vertically as well as laterally away from the channel. The erosional bases of the lenticular bedforms indicates that flows exerted a high shear stress on the bed, high enough to erode into apparently consolidated mudstones (Figures 7 and 8). The erosion surface is, in places, undular and cuts through the mudstones and thin-bedded turbidites at low angles, suggesting that these layers were reasonably consolidated (Figure 7). The broad, undulating erosion surface is superimposed with small-scours, which are filled with coarser sediment (Figure 8). The scours presumably developed from some local bed defect (Allen, 1971) and this process probably acted as a seed point for the low-amplitude erosion surfaces that characterize the base of these bedforms.

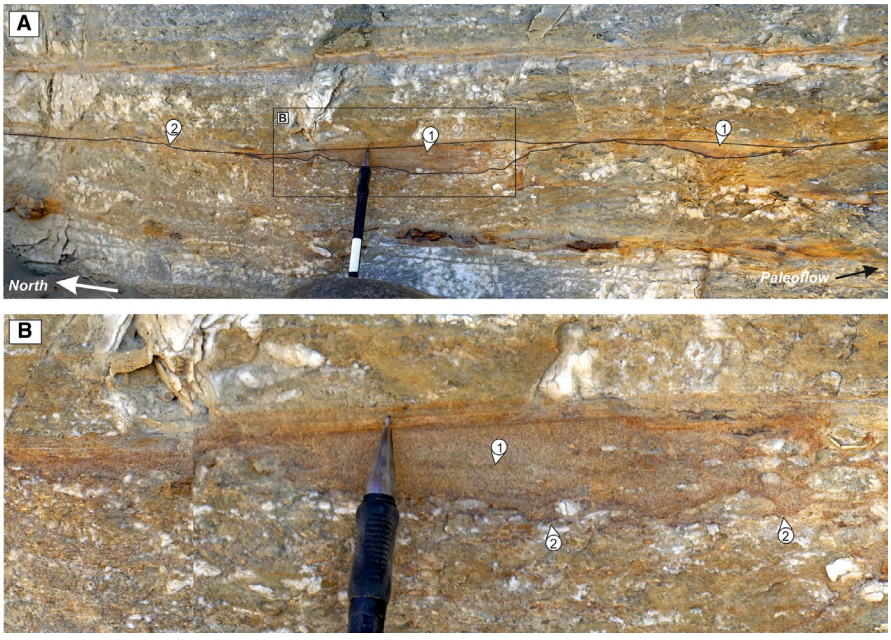

FIGURE 8 (A) Small-scours (1) associated with an overbank erosion/bypass surface (2). The box marks the inset 'B'. (B) The scours trapped and preserved some of the sediment of the dominantly bypassing flow. The fill of these features is either marked by downstream (SE) dipping laminae (1), which is to the right in the images, or can be massive. In these examples, the basal erosion surface is intricate with contemporaneous small-scale injection into the lateral and basal margins of the scour (2)

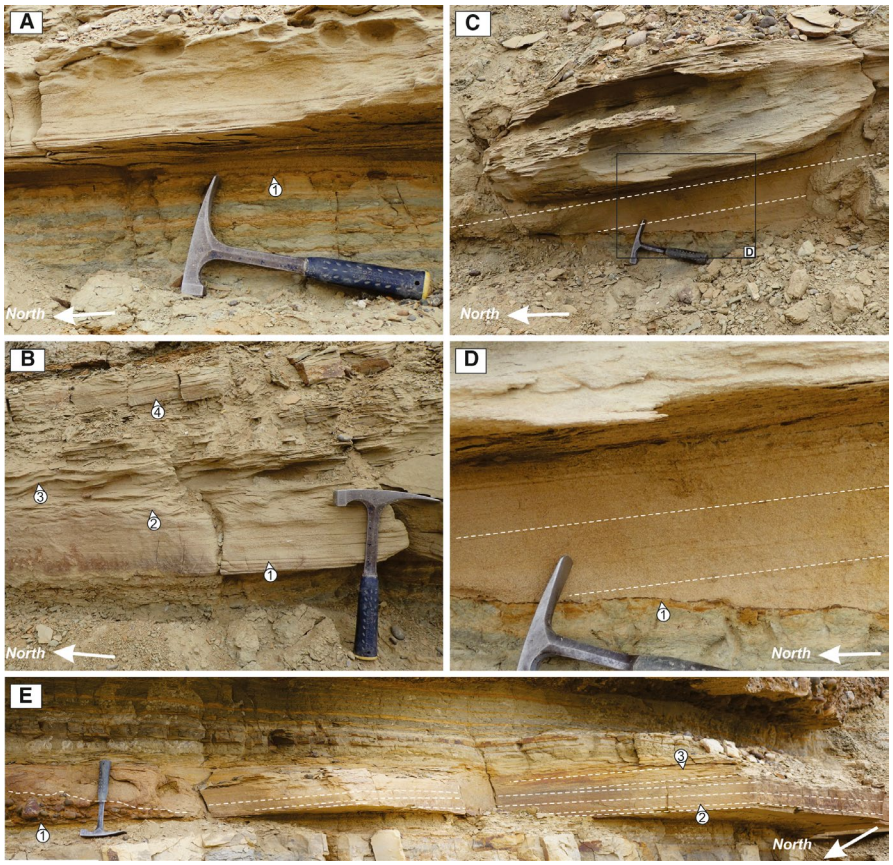

FIGURE 9 Details of bedforms: (A) Low angle backsets overlying an irregular erosion surface. (1). (B) Wedge-like geometry of bedform with low angle backsets at base (1), overlain by subcritical, (2) then supercritical climbing ripples (3) and planar lamination (4). (C) Steep backsets overlain by subcritical climbing ripples. (D) Detail of steep backsets overlying an irregular erosion surface (1). (E) Detail of bed 2 from Figure 4. The bed extends from a conglomerate wing (1); note the low angle backsets rising away from the conglomerate (2) and climbing ripples (3)

The sediment overlying the erosion surface is variable depending on its position with respect to the crest of the overlying bedform (Figure 7). This presumably relates to the concentration of the flow, its duration and distance from its parent channel when the sediment was deposited. Where coarse material filling a scour is directly overlain by mudstone, demonstrating missing grain size fractions (Figure 8), bypass of the fine tail of the turbidity current is implied. The presence of stranded coarse particles and clasts in the bedforms suggests that clasts may have been deposited as part of a wider splay from the channel, but that these are winnowed remnants. In the thickest part of the bedforms, in some cases, the deposit is characterized by backset bedding (Figure 9). Backsets are thought to develop under flow conditions approaching, at, or above Froude unity, that is, supercritical flow, or by a flow passing through a hydraulic jump (Jopling and Richardson, 1966; Skipper, 1971; Schmincke et al., 1973; Skipper and Bhattacharjee, 1978; Postma and Cartigny, 2014). Therefore, the lower part of these bedforms is interpreted to indicate the occurrence of Froude-supercritical flow; such conditions existed in the channel during gravel transport, probably across the overbank during the formation of the basal erosion surface, and during the development of the backset bedding (Figure 11). Hypothetical velocity profiles may help

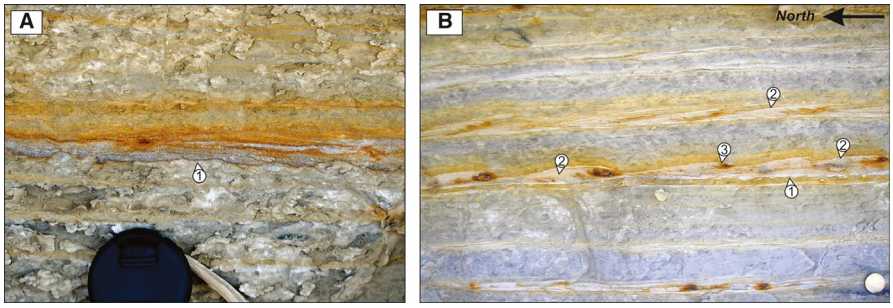

FIGURE 10 Ripples with erosional bases. (A) Supercritical climbing ripples with intricate erosional surfaces at their bases (1). (B) Subcritical climbing ripples with a low angle erosion surface at their base (1); these ripples commonly have slightly overturned foresets (2) and are marked by dewatering on their lee-sides, with iron cement picking out the slightly higher permeability zone (3). $10 Peso coin for scale (28 mm diameter)

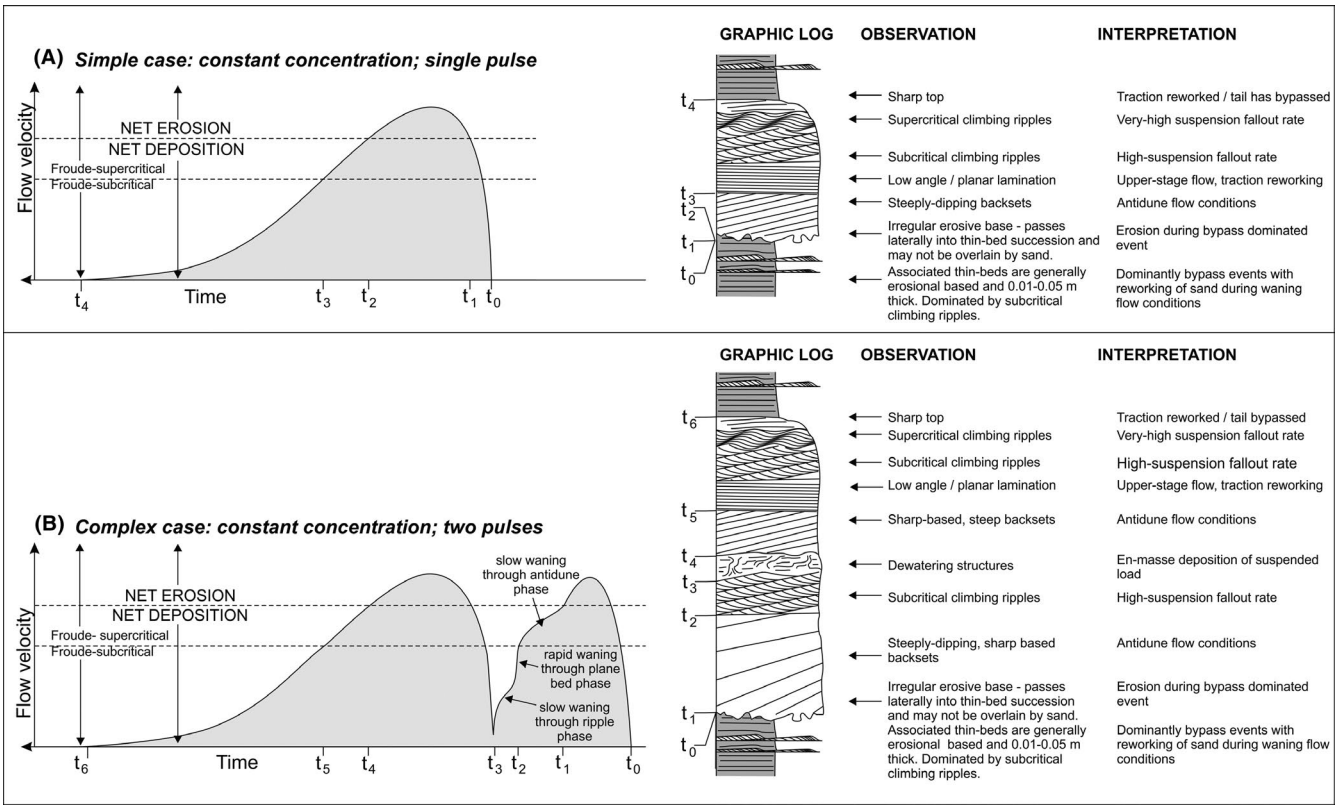

FIGURE 11 Schematic velocity profiles illustrating the evolution of overbank flows based on sedimentary structures. (A) Simple waning flow and characteristic bed profile. (B) Suggested velocity profile for repeated facies stack of Bed 1 in Figure 5 with the observed bed profile. Timescale is not necessarily linear and although simplifying, profiles assume a constant flow thickness and concentration

us to explain the development of the observed bedforms and the switch from Froude-supercritical to subcritical flow conditions (Figure 11). The sequence of scour, initial formation of deposits by Froude-supercritical flow and subsequently subcritical flow cannot be explained purely by changes in the flow structure. Interaction with a developing seafloor, as proposed by Massari (1996, 2017) to describe scour fills (albeit in a different depositional environment), with a locally fixed hydraulic jump within the scour, would allow for the transition from Froude-supercritical to subcritical flow conditions.

Through time flow strength waned as recorded by the sedimentary structures (Figures 9 and 11). However, a simple waning profile is not always present; there may be internal erosion surfaces and repetition of facies successions indicating rejuvenation of flow energy (Stevenson et al., 2015). Such pulsing flows may be characteristic of overspilling channelized flows (Normark, 1989; Kane et al., 2010b). Similar records of pulsing has been reported from modern flows (Best et al., 2005), from the geological record of internal levees (Kane et al., 2009, 2010a; Kane and Hodgson, 2011), and depositional terraces (Hansen et al., 2015). Where a coarse-grained lag is present, it is inferred that multiple flows may have been responsible for formation of the bedforms. However, it cannot be unequivocally reconciled whether repeated, rapidly recurring flows of a similar capacity or pulsating flows generated these bedforms. The development of the bedforms may be linked to a number of mechanisms (e.g. antidunes or cyclic-steps) and is discussed below.

5 | DISCUSSION

5.1 | Comparison to other overbank sand bars and bedforms

'Sediment wave' is a term generally reserved for much larger features that are commonly observed associated with submarine channel-levees in seismic data and on the seafloor, often tens of metres high and hundreds of metres long (Wynn et al., 2002; Symons et al., 2016). In visualizations of seismic data, they are typically formed of transparent or dim reflectors that contrast sharply with the stronger amplitudes encountered in channel-fills (Normark et al., 2002). They are consequently interpreted as being fine-grained (clay-silt), deposited by turbidity currents overspilling the channel and potentially amplified by bottom currents (Normark et al., 2002; Wynn et al., 2002). Features of the scale illustrated herein are typically not captured by seismic or seafloor images. Although

discontinuous units have been recognized in outcropping levees (Khan et al., 2011; Hansen et al., 2017), limited attention has been paid to the consistency of individual beds.

These features are closer to the scale of overbank sandstone lenses described by Campion et al. (2011) who reported lenticular sandstones from the Cretaceous Cerro Toro Formation, which are slightly larger (up to 1.5 m thick, at least 50 m long) than the features described here but are interpreted to have developed in a similar depositional setting. The lenses described from the Cerro Toro Formation developed in troughs between fine-grained siltstone topography, interpreted to represent overbank bedforms, with the sandstones essentially ponded between bedform crests. The resulting sedimentary structures show Bouma Ta-Tb divisions and mud-clast horizons. In the present case, there is no basal topography confining the sandstone lenses apart from minor erosional relief, and the bedforms are aggradational, forming rather than filling topographic features (Figure 4). Therefore, despite being of a similar scale, they have quite different origins and significance, being attributed to waning currents overspilling from a nearby channel (Campion et al., 2011).

Small (centimetre scale), siltstone-dominated dunes developed on the flanks of external levees have been reported from the Fort Brown Formation (Morris et al., 2014). Those aggradational bedforms developed sinusoidal cross-sectional geometries and may be relatively straight-crested (although constrained by limited bedding plane exposures), with crests sub-parallel to the channel margin. These are relatively small compared to the bedforms in the Rosario Formation and were interpreted as developing beneath Froude-subcritical flows.

In terms of facies, perhaps the closest comparison can be made with the sandy 'sediment waves' of the Miocene Cabo Viamonte Beds (Tierra Del Fuego), which were interpreted as base of (clinoform) slope hyperpycnal flow deposits (Ponce and Carmona, 2011). These bedforms are of similar dimensions to those recorded here, although the present examples are at the smaller end of the size spectrum, and they have an erosional base which is overlain by a similar facies stack. The centres of the bedforms are dominated by up current dipping foresets with gravelly intercalations. Ponce and Carmona's (2011) model is one of waxing then waning flow, with the coarsest sediment deposited early, then reworked by erosive flows; this contrasts with the present model of highest energy flow at the onset, forming the erosion surface prior to deposition in an essentially waning flow (Figure 11). The heterolithic deposits within which they are inter-bedded drape and thicken between waves, as observed here (Figure 7). These are similar in terms of the deposit, but occur within a different interpreted depositional environment and are attributed to hyperpycnal turbidity currents.

Coarse-grained antidune bedforms have been described from several deep-marine channel outcrops (Ito and Saito, 2006; Ito, 2010; Lang et al., 2017), but were first described by Winn and Dott (1977) from the Lago Sofia conglomerates of the Cerro Toro, Formation. There, large gravel-bedforms, up to 4 m in height, with prominent backset bedding were interpreted to have developed under antidune flow conditions. These examples are all coarser grained, show different vertical trends in sedimentary structures, are larger scale than the examples reported here and being from within channels they do not represent overbank sediments.

Coarse-grained sediment waves and bars have also been described from studies of the modern seafloor (Piper et al., 1985; Wynn et al., 2002; Paull et al., 2011; Gamberi et al., 2013; Kostic, 2014; Covault et al., 2017; Hage et al., 2018). These are typically larger than the bedforms described here, with wavelengths on the order of tens to hundreds of metres and heights from 1 to 10 m. These features are generally interpreted as antidunes or cyclic-steps formed under Froude-supercritical flow (Wynn et al., 2002; Postma and Cartigny, 2014).

In summary, the bedforms described here may have previously been overlooked in outcrop studies or are simply not present. They are typically smaller and finer grained than the gravelly sediment waves reported from a number of seafloor studies, from a few outcrops and orders of magnitude smaller than typical fine-grained sediment waves on channel-levees. These bedforms formed partially under Froude-supercritical flow conditions suggesting that they were not formed by internal lee waves (Flood, 1988; Kneller and Buckee, 2000). They are also below the scale of deposits documented from lee waves and cyclic-steps (Cartigny et al., 2011). Therefore, their formation is attributed to antidune flow conditions, which formed as turbidity currents overspilled from a channel, eroded and then deposited sediment in the overbank area, followed by a transition to Froude-subcritical flow conditions as the overspilling current waned (Figure 12).

5.2 | Contemporaneous development of the channel-fill and overbank succession

An important implication of the recognition of overbank bedforms related directly to bypass-dominated channelized flows is that aggradation of the overbank succession can potentially be directly tied to the evolution of the channel. If the favoured interpretation is correct, it demonstrates that low-relief (internal levee or depositional terrace) confinement was developing contemporaneously with channel-fill aggradation. In the Isaac Channel 3 of the Neoproterozoic Isaac Formation, Canada, channel migration is recorded by events which were erosional into the outer bend overbank deposits, resulting in splay deposits, also demonstrating contemporaneous levee-channel-fill aggradation, albeit in a punctuated

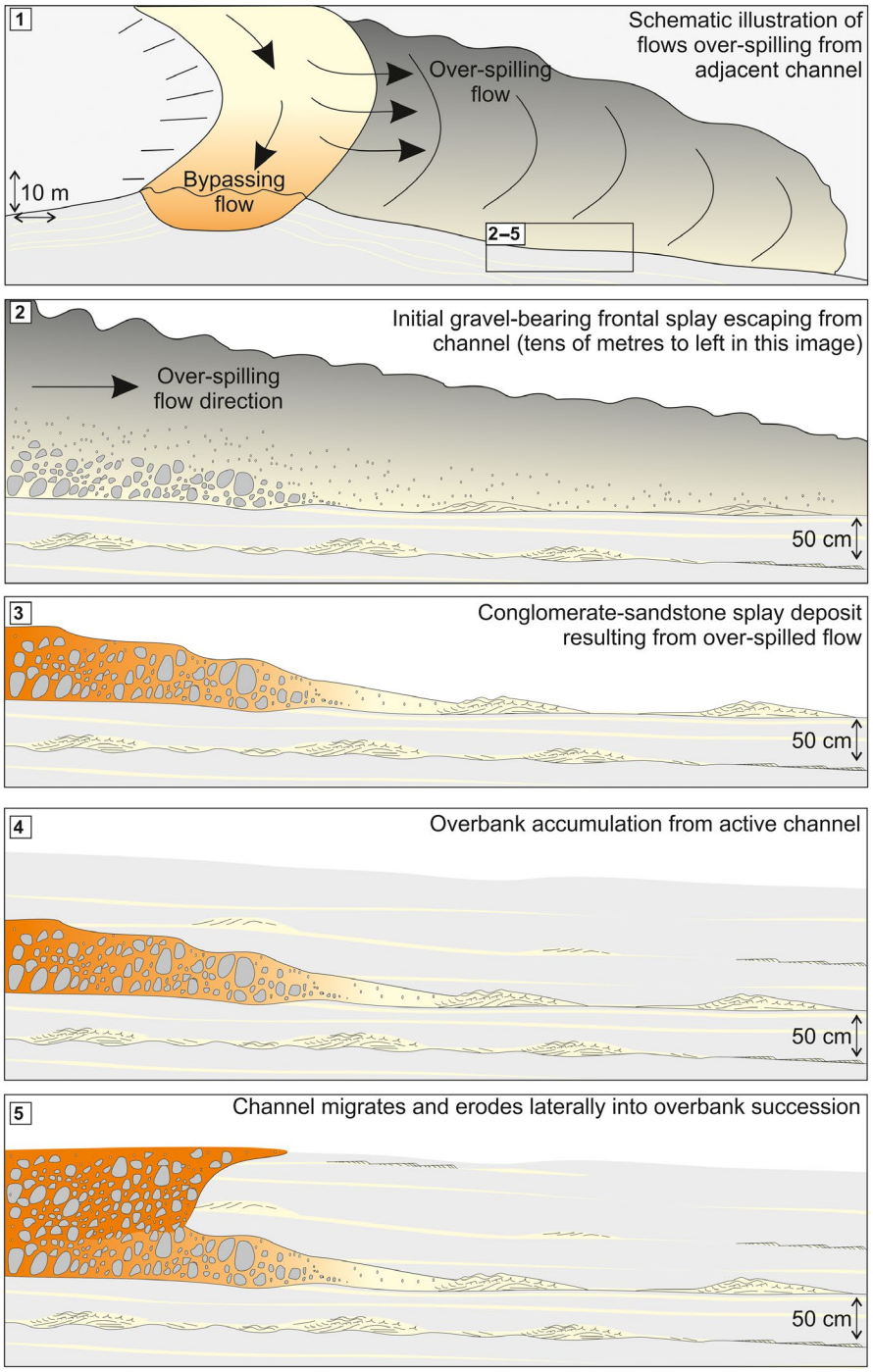

FIGURE 12 (1) Schematic illustration of channel–levee system with overspilling flows, evolution of which is demonstrated in schematic cross-sections (2–5), showing the evolution of the overbank bedforms and bypass surfaces in successions laterally adjacent to active channels

fashion (Khan and Arnott, 2011). Contemporaneous inner bend accumulation of levee deposits associated with lateral-accretion has also been reported from the Isaac Channel 2 (Arnott, 2007).

In contrast, external levees or internal levees developed adjacent to entrenched channels may develop during periods of channel-bypass and not tie directly to the channel-fill, as has been demonstrated for the Eocene–Oligocene Tinker Channel, Turkey (Cronin et al., 2000) and in the Permian Fort Brown Formation, South Africa (Di Celma et al., 2011; Brunt et al., 2013; Morris et al., 2014). The contemporaneous nature of the deposits described here contrasts to the external levee of the San Fernando system where the boundary with adjacent channel-belt fill is diachronous (Kane et al., 2007). The lowermost part of the S-channel-fill, above the initial conglomeratic deposits, is marked by at least a several hundred metre wide belt of lateral migration, suggesting that during these phases, when conglomerate deposition was focused on the inner bank, finer sediments accumulated on the overbank. Erosion of overbank deposits occurred during

channel migration, whilst anomalously large flows that covered a wider area were able to transport gravel onto the overbank, creating thin gravel wings (e.g. Figure 6). The model is summarized in Figure 12.

5.3 | Recognition in core and significance to hydrocarbon exploration and production

The sedimentary bodies described are distinctive, and when paired with an interpretation of their palaeoenvironmental context, they should be recognizable in core. A series of schematic vertical core profiles illustrating the range of likely expressions of these bedforms in the subsurface is presented (Figure 13). Where recognized, either in outcrop, core, or with borehole image logs, they are potentially an indicator of proximity to a channel that was contemporaneously active and bypassing sediment down-dip, allowing the prediction of the likelihood of reservoir bodies, potentially both laterally and down-dip. The presence of these sandstone bedforms may also enhance the overall net-to-gross of overbank deposits, often considered as poor or non-reservoir. The recognition of this facies association does not provide a unique interpretation but should be considered in view of its context. Similar facies associations, with a partial or complete sequence of structures, may be anticipated in any environment where bypass conditions predominate, for example, within the channel and at channel-lobe transitions.

6 | CONCLUSIONS

This study documents lenticular sandstones that are interpreted to represent overbank bedforms within a thin-bedded interval of channel-belt deposits. Bedforms of this scale have not previously been recorded in the literature and have the following features (Figure 11):

- An erosional base that can pass into a laterally continuous erosion surface, which can be relatively undulose. The longer wavelength erosion surfaces can be intricate but lack loading structures, suggesting that the substrate had some strength at the time of erosion. Where sand was not deposited (or preserved) above the erosion surface, it may be

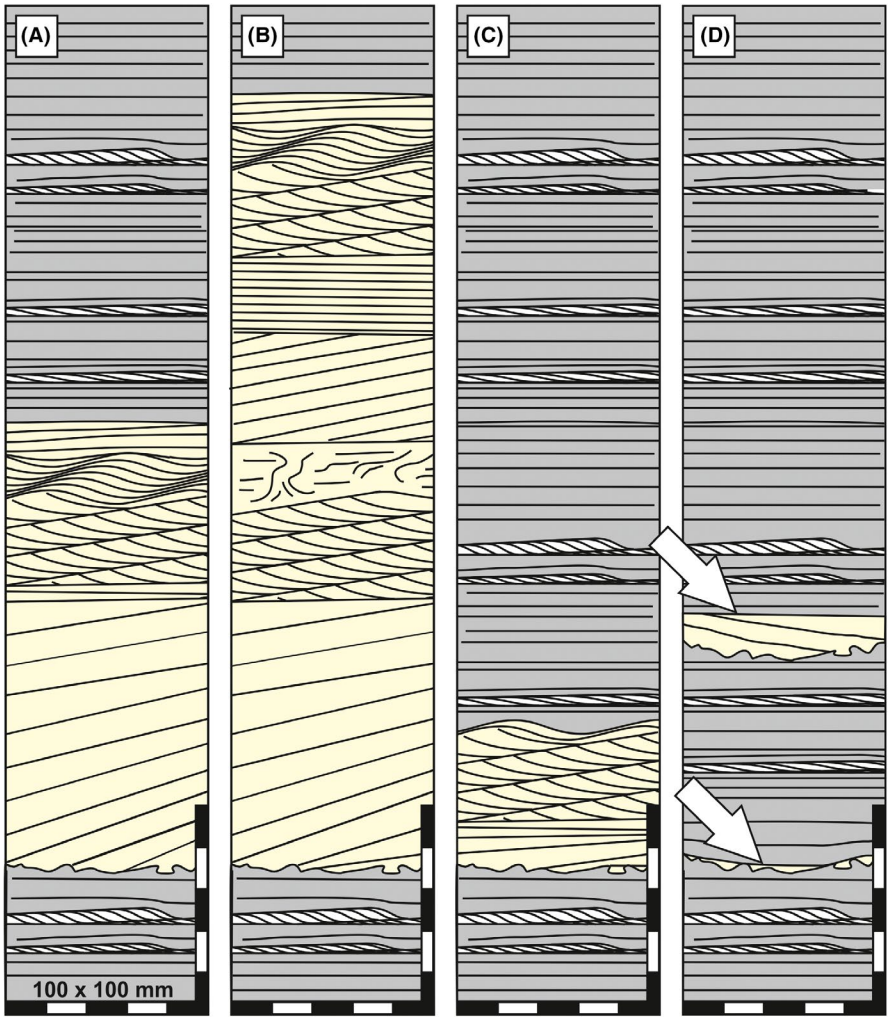

FIGURE 13 Illustrations of overbank sandstone bedforms in core (highlighted in yellow). (A) Typical bedform illustrating simple waning flow; (B) repeated facies stack illustrating rejuvenation of flow strength; (C) intersection through the toe of a sandstone bedform; (D) sandstone lenses developed in erosional topography during bypass-dominated event – two examples are illustrated (arrowed)

overlain by siltstone or finer sediment. Small-scours may be filled with coarse sandstone and lacking the finer component, indicating its origin as a winnowed bypass lag.
- This erosional base may originate within the conglomeratic channel-fill, grading laterally into the sandstone bedforms.
- A complex stack of sedimentary structures, indicative of Froude-supercritical and subcritical flow and increasing sediment fallout rate are described. Although there is variability within and between bedforms, a typical bedform has the following vertical stacking pattern from the erosional base:
  - Planar backsets representing antidune upper stage flow conditions; these can be nearly horizontal, to relatively steep (10°).
  - Planar lamination representing upper stage flow.
  - Subcritically climbing ripples representing lower stage flow and high suspended load fallout rate.
  - Supercritically climbing ripples representing lower stage flow and increased sediment fallout rate.
  - Sinusoidal to lower stage lamination, representing high fallout rates and reduced shear stress.
  - A sharp top, indicating the top is reworked and flow was ongoing.
- Repeated facies stacks of individual bedforms record rejuvenation of overspill energy, which is a common feature previously noted in internal levee deposits.
- Although typically considered an area dominated by simple, waning flows, this study demonstrates a range of flow processes to have been active in deep-water channel overbank settings (Figure 11).
- The bedforms are developed in a succession of overbank deposits that accumulated, at least in part, contemporaneously with the actively migrating channel (Figure 12).
- Such features may provide useful diagnostic tools in the interpretation of thin-bedded channelized environments in the subsurface (Figure 13).

ACKNOWLEDGEMENTS

The authors acknowledge the support of the PRACSS Joint Industry Project at the University of Aberdeen, funded by BP, AkerBP, Equinor and Petrochina, which has allowed us to undertake this research. We also thank Amanda Santa Catharina for field assistance. Chris Stevenson and an anonymous reviewer are thanked for their constructive reviews and Editor Peter Swart is thanked for handling this article. We also thank Bill Arnott, Matthieu Cartigny and William McCaffrey for reviewing a previous version of this manuscript.

CONFLICT OF INTEREST

We have no conflict of interest to declare.

ORCID


Adam McArthur https://orcid.org/0000-0002-7245-9465

REFERENCES

Alexadri-Rionda, R., Martínez-Vera, A., Espinosa-Aramburu, E.G., Terán-Ortega, L.A., Maraver-Romero, D.V. and Arriaga-Meléndez, H. (2008) *Carta Geológico-Minera Estado de Baja California, 1: 500000: Distrito Federal*. México: Servicio Geológico Mexicano, Secretaria de Economía, p. 1.

Allen, J.R.L. (1971) Transverse erosional marks of mud and rock: their physical basis and geological significance. *Sedimentary Geology*, *5*(3–4), 167–385

Allen, J.R.L. (1982) *Sedimentary structures, their character and physical basis (Vol. 1)*. Developments in Sedimentology, 30A. Amsterdam: Elsevier, 593 p.

Arnott, R.W.C. (2007) Stratal architecture and origin of lateral accretion deposits (LADs) and conterminous inner-bank levee deposits in a base-of-slope sinuous channel, lower Isaac Formation (Neoproterozoic), East-Central British Columbia, Canada. *Marine and Petroleum Geology*, *24*(6–9), 515–528

Babonneau, N., Savoye, B., Cremer, M. and Bez, M. (2004)Multiple terraces within the deep incised Zaire Valley (ZaïAngo Project): are they confined levees? In: S. A. Lomas, & P. Joseph (Eds.), *Confined turbidite systems*. *Geological Society, London, Special Publications*, *222*(1), 91–114.

Beal, C.H. (1948) Reconnaissance of the geology and oil possibilities of Baja California, Mexico. *Geological Society of America Memoir*, *31*, 138.

Best, J.L., Kostaschuk, R.A., Peakall, J., Villard, P.V. and Franklin, M. (2005) Whole flow field dynamics and velocity pulsing within natural sediment-laden underflows. *Geology*, *33*(10), 765–768

Brunt, R.L., Di Celma, C.N., Hodgson, D.M., Flint, S.S., Kavanagh, J.P. and van der Merwe, W.C. (2013) Driving a channel through a levee when the levee is high: An outcrop example of submarine down-dip entrenchment. *Marine and Petroleum Geology*, *41*, 134–145

Buffington, E.C. (1952) Submarine 'natural levees'. *Journal of Geology*, *60*, 473–479.

Busby, C., Smith, D., Morris, W. and Fackler-Adams, B. (1998) Evolutionary model for convergent margins facing large ocean basins: Mesozoic Baja California, Mexico. *Geology*, *26*, 227–230

Callow, R.H.T., McIlroy, D., Kneller, B. and Dykstra, M. (2013) Integrated ichnological and sedimentological analysis of a Late Cretaceous submarine channel-levee system: The Rosario Formation, Baja California, Mexico. *Marine and Petroleum Geology*, *41*, 277–294. https://doi.org/10.1016/j.marpetgeo.2012.02.001

Campion, K.M., Dixon, B.T. and Scott, E.D. (2011) Sediment waves and depositional implications for fine-grained rocks in the Cerro Toro Formation (upper Cretaceous), Silla Syncline, Chile. *Marine and Petroleum Geology*, *28*, 761–784.

Cartigny, M.J., Postma, G., van den Berg, J.H. and Mastbergen, D.R. (2011) A comparative study of sediment waves and cyclic steps based on geometries, internal structures and numerical modeling. *Marine Geology*, *280*, 40–56

Di Celma, C., Brunt, R., Hodgson, D., Flint, S. and Kavanagh, J. (2011) Spatial and temporal evolution of a Permian submarine slope channel-levee system, Karoo Basin, South Africa. *Journal of Sedimentary Research*, *81*, 579–599

Collinson, J.D. and Thompson, D.B. (1982) *Sedimentary structures*. London, UK: George, Allen & Unwin, LtD, 244 pp.

Covault, J.A., Kostic, S., Paull, C.K., Sylvester, Z. and Fildani, A. (2017) Cyclic steps and related supercritical bedforms: building blocks of deep-water depositional systems, western North America. *Marine Geology*, *393*, 4–20

Cronin, B.T., Hurst, A., Celik, H. and Türkmen, I. (2000) Superb exposure of a channel, levee and overbank complex in an ancient deep-water slope environment. *Sedimentary Geology*, *132*, 205–216.

Crowell, J.C. (1957) Origin of pebbly mudstones. *Geological Society of America Bulletin*, *68*, 993–1010.

Dykstra, M. and Kneller, B. (2007) Canyon San Fernando: A deep-marine channel-Levee complex exhibiting evolution from submarine canyon-confined to unconfined. In: Nilson, T., Shew, R., Steffens, G. and Studlick, J. (Eds.) *AAPG Atlas of Deepwater Outcrops*. Tulsa, OK: American Association of Petroleum Geologists Special Publications, pp. 226–229.

Dykstra, M. and Kneller, B. (2009) Lateral accretion in a deep-marine channel complex: implications for channellized flow processes in turbidity currents. *Sedimentology*, *56*, 1411–1432. https://doi.org/10.1111/j.1365-3091.2008.01040.x

Ercilla, G., Alonso, B., Wynn, R.B. and Baraza, J. (2002) Turbidity current sediment waves on irregular slopes: observations from the Orinoco sediment–wave field. *Marine Geology*, *192*, 171–187.

Flood, R.D. (1988) A lee wave model for deep-sea mudwave activity. *Deep Sea Research Part A. Oceanographic Research Papers*, *35*, 973–983

Gamberi, F., Rovere, M., Dykstra, M., Kane, I. and Kneller, B. (2013) Integrating modern seafloor and outcrop data in the analysis of slope channel architecture and fill. *Marine and Petroleum Geology*, *41*, 83–103. https://doi.org/10.1016/j.marpetgeo.2012.04.002

Gastil, R.G., Philips, R.C. and Allison, E.C. (1975) Reconnaissance geology of the state of Baja California. *Geological Society of America Memoirs*, *140*, 170.

Hage, S., Cartigny, M.J., Clare, M.A., Sumner, E.J., Vendettuoli, D., Hughes Clarke, J.E., et al. (2018) How to recognize crescentic bedforms formed by supercritical turbidity currents in the geologic record: Insights from active submarine channels. *Geology*, *46*, 563–566

Hansen, L.A.S., Callow, R.H.T., Kane, I.A., Gamberi, F., Rovere, M., Cronin, B.T. et al. (2015) Genesis and character of thin-bedded turbidites associated with submarine channels. *Marine and Petroleum Geology*, *67*, 852–879.

Hansen, L.A.S., Callow, R., Kane, I.A. and Kneller, B.C. (2017) Differentiating submarine channel related thin-bedded turbidite facies: Outcrop example from the Rosario Formation, Mexico. *Sedimentary Geology*, *358*, 19–34.

Huang, H., Imran, J., Pirmez, C., Zhang, Q. and Chen, G. (2009) The critical densimetric Froude number of subaqueous gravity currents can be non-unity or non-existent. *Journal of Sedimentary Research*, *79*, 479–485.

Hughes Clarke, J.E. (2016) First wide-angle view of channelized turbidity currents links migrating cyclic steps to flow characteristics. *Nature Communications*, *7*, 11896.

Ito, M. (2010) Are coarse-grained sediment waves formed as downstream-migrating antidunes? Insight from an early Pleistocene submarine canyon on the Boso Peninsula, Japan. *Journal of Sedimentary Research*, *226*, 1–8.

Ito, M. and Saito, T. (2006) Gravel waves in an ancient canyon: analogous features and formative processes of coarse-grained bedforms in a submarine-fan system, the lower Pleistocene of the Boso Peninsula, Japan. *Journal of Sedimentary Research*, *76*, 1274–1283.

Jopling, A.V. and Richardson, E.V. (1966) Backset bedding developed in shooting flow in laboratory experiments. *Journal of Sedimentary Petrology*, *36*, 821–825.

Kane, I.A. and Hodgson, D. (2011) Sedimentological criteria to differentiate submarine channel levee subenvironments: Exhumed examples from the Rosario Fm. (Upper Cretaceous) of Baja California, Mexico, and the Fort Brown Fm. (Permian), Karoo Basin, S. Africa. *Marine and Petroleum Geology*, *28*, 807–823. https://doi.org/10.1016/j.marpetgeo.2010.05.009

Kane, I.A., Kneller, B.C., Dykstra, M., Kassem, A. and McCaffrey, W.D. (2007) Anatomy of a submarine channel-levee: An example from Upper Cretaceous slope sediments, Rosario Formation, Baja California, Mexico. *Marine and Petroleum Geology*, *24*, 540–563. https://doi.org/10.1016/j.marpetgeo.2007.01.003

Kane, I.A., Dykstra, M., Kneller, B.C., Tremblay, S. and McCaffrey, W.D. (2009) Architecture of a coarse grained channel-levee system: the Rosario Formation, Baja California, Mexico. *Sedimentology*, *56*, 2207–2234.

Kane, I.A., McCaffrey, W.D., Peakall, J. and Kneller, B.C. (2010a) Submarine channel levee shape and sediment waves from physical experiments. *Sedimentary Geology*, *223*, 75–85.

Kane, I.A., McCaffrey, W.D. and Peakall, J. (2010b) On the origin of paleocurrent complexity in deep marine channel-levees. *Journal of Sedimentary Research*, *80*, 54–66.

Khan, Z.A. and Arnott, R.W.C. (2011) Stratal attributes and evolution of asymmetric inner- and outer-bend levee deposits associated with an ancient deep-water channel-levee complex within the Isaac Formation, southern Canada. *Marine and Petroleum Geology*, *28*, 824–842.

Khan, Z.A., Arnott, B. and Pugin, A. (2011) An alternative model of producing topography in the crest region of deep-water levees. *American Association of Petroleum Geologists Bulletin*, *95*, 2085–2106.

Kneller, B. (1995) Beyond the turbidite paradigm: Physical models for deposition of turbidites and their implications for reservoir prediction. In: A. J. Hartley, & D. J. Prosser (Eds), *Characterization of Deep Marine Clastic Systems*. *Geological Society of London Special Publication*, *94*, 31–49.

Kneller, B. (2003) The influence of flow parameters on turbidite slope channel architecture. *Marine and Petroleum Geology*, *20*, 901–910.

Kneller, B.C., Bozetti, G., Callow, R., Dykstra, M., Hansen, L., Kane, I., et al. (2019) Architecture, process and environmental diversity in a Late Cretaceous slope channel system. *Journal of Sedimentary Research*, in press.

Kneller, B.C. and Branney, M.J. (1995) Sustained high density turbidity currents and the deposition of thick massive sands. *Sedimentology*, *42*, 607–616.

Kneller, B. and Buckee, C. (2000) The structure and fluid mechanics of turbidity currents: a review of some recent studies and their geological implications. *Sedimentology*, *47*, 62–94.

Komar, P.D. (1973) Continuity of turbidity current flow and systematic variations in deep-sea channel morphology. *Geological Society of America Bulletin*, *84*, 3329–3338.

Kostic, S. (2011) Modeling of submarine cyclic steps: Controls on their formation, migration, and architecture. *Geosphere*, *7*, 294–304.

Kostic, S. (2014) Upper flow regime bedforms on levees and continental slopes: Turbidity current flow dynamics in response to fine-grained sediment waves. *Geosphere*, *10*, 1094–1103.

Lang, J., Brandes, C. and Winsemann, J. (2017) Erosion and deposition by supercritical density flows during channel avulsion and backfilling: Field examples from coarse-grained deepwater channel-levée complexes (Sandino Forearc Basin, southern Central America). *Sedimentary Geology*, *349*, 79–102.

Leclair, S.F. and Arnott, R.W.C. (2005) Parallel lamination formed by high-density turbidity currents. *Journal of Sedimentary Research*, *75*, 1–5.

Lewis, K.B. and Pantin, H.M. (2002) Channel-axis, overbank and drift sediment waves in the southern Hikurangi Trough, New Zealand. *Marine Geology*, *192*, 123–151.

Li, P., Kneller, B.C., Thompson, P., Bozetti, G. and Dos Santos, T. (2018) Architectural and facies organisation of slope channel fills: Upper Cretaceous Rosario Formation, Baja California, Mexico. *Marine and Petroleum Geology*, *92*, 632–649.

Lowe, D.R. (1975) Water escape structures in coarse-grained sediments. *Sedimentology*, *22*, 157–204.

Lowe, D.R. (1982) Sediment gravity flows; II, Depositional models with special reference to the deposits of high-density turbidity currents. *Journal of Sedimentary Research*, *52*, 279–297.

Lowe, D.R. (1988) Suspended-load fallout rate as an independent variable in the analysis of current structures. *Sedimentology*, *35*, 765–776.

Massari, F. (1996) Upper-flow-regime stratification types on steep-face, coarse-grained, Gilbert-type progradational wedges (Pleistocene, southern Italy). *Journal of Sedimentary Research*, *66*, 364–375.

Massari, F. (2017) Supercritical-flow structures (backset-bedded sets and sediment waves) on high-gradient clinoform systems influenced by shallow-marine hydrodynamics. *Sedimentary Geology*, *360*, 73–95.

McArthur, A.D., Kneller, B.C., Souza, P.A. and Kuchle, J. (2016) Characterization of deep-marine channel-levee complex architecture with palynofacies: An outcrop example from the Rosario Formation, Baja California, Mexico. *Marine and Petroleum Geology*, *73*, 157–173.

Menard, H.W. (1955) Deep-sea channels, topography, and sedimentation. *American Association of Petroleum Geologists Bulletin*, *39*, 236–255.

Morris, W. and Busby-Spera, C.J. (1988) Sedimentologic Evolution of a Submarine Canyon in a Forearc Basin, Upper Cretaceous Rosario Formation, San Carlos, Mexico. *American Association of Petreoleum Geologists Bulletin*, *72*, 717–737.

Morris, W. and Busby-Spera, C.J. (1990) A submarine-fan valley-levee complex in the Upper Cretaceous Rosario Formation: Implication for turbidite facies models. *Geolgical Society of America Bulletin*, *102*, 900–914.

Morris, E., Hodgson, D., Brunt, R. and Flint, S. (2014) Origin, evolution and anatomy of silt-prone submarine external levées. *Sedimentology*, *61*, 1734–1763. https://doi.org/10.1111/sed.12114

Normark, W.R. (1989) Observed parameters for turbidity-current flow in channels, Reserve Fan, Lake Superior. *Journal of Sedimentary Research*, *59*, 423–431.

Normark, W.R., Hess, G.R., Stow, D.A.V. and Bowen, A.J. (1980) Sediment waves on the Monterey Fan levee: a preliminary physical interpretation. *Marine Geology*, *37*, 1–18.

Normark, W.R., Piper, D.J.W. and Stow, D.A.V. (1983) Quaternary development of channels, levees, and lobes on middle Laurentian Fan. *American Association of Petroleum Geologists Bulletin*, *67*, 1400–1409.

Normark, W.R., Piper, D.J., Posamentier, H., Pirmez, C. and Migeon, S. (2002) Variability in form and growth of sediment waves on turbidite channel levees. *Marine Geology*, *192*, 23–58.

Paull, C.K., Caress, D.W., Ussler, W., Lundsten, E. and Meiner-Johnson, M. (2011) High-resolution bathymetry of the axial channels within Monterey and Soquel submarine canyons, offshore central California. *Geosphere*, *7*, 1077–1101.

Peakall, J., McCaffrey, B. and Kneller, B. (2000) A process model for the evolution, morphology, and architecture of sinuous submarine channels. *Journal of Sedimentary Research*, *70*, 434–448.

Piper, D.J.W. and Normark, W.R. (1983) Turbidite depositional patterns and flow characteristics, Navy submarine fan, California Borderland. *Sedimentology*, *30*, 681–694.

Piper, D.J.W., Shor, A.N., Farre, J.A., O'Connell, S. and Jacobi, R. (1985) Sediment slides and turbidity currents on the Laurentian Fan: Sidescan sonar observations near the epicenter of the 1929 Grand Banks earthquake. *Geology*, *13*, 538–541.

Ponce, J.J. and Carmona, N. (2011) Coarse-grained sediment waves in hyperpycnal clinoform systems, Miocene of the Austral foreland basin, Argentina. *Geology*, *39*, 763–766.

Postma, G. and Cartigny, M. (2014) Supercritical and subcritical turbidity currents and their deposits – A synthesis. *Geology*, *42*, 987–990.

Postma, G., Nemec, W. and Kleinspehn, K.L. (1988) Large floating clasts in turbidites: a mechanism for their emplacement. *Sedimentary Geology*, *58*, 47–61

Rees, A.I. (1968) The production of preferred orientation in a concentrated dispersion of elongated and flattened grains. *Journal of Geology*, *76*, 457–465.

Rees, A.I. (1983) Experiments on the production of transverse grain alignment in a sheared dispersion. *Sedimentology*, *30*, 437–448.

Røe, S.L. and Hermansen, M. (2006) New aspects of deformed cross-strata in fluvial sandstones: examples from Neoproterozoic formations in northern Norway. *Sedimentary Geology*, *186*, 283–293.

Schmincke, H.-U., Fisher, R.V. and Waters, A.C. (1973) Antidune and chute and pool structures in the base surge deposits of the Laacher See area, Germany. *Sedimentology*, *20*, 553–574

Skipper, K. (1971) Antidune cross-stratification in a turbidite sequence, Cloridorme Formation (Middle Ordovician) Gaspé, Quebec. *Sedimentology*, *20*, 553–574.

Skipper, K. and Bhattacharjee, S.B. (1978) Backset bedding in turbidites: a further example from the Cloridorme Formation (Middle Ordovician), Gaspé, Quebec. *Journal of Sedimentary Petrology*, *48*, 193–202.

Sprague, A. R., Sullivan, M. D., Campion, K. M., Jensen, G. N., Goulding, F. J., Garfield, T. R. et al. (2002) The physical stratigraphy of deep-water strata: A hierarchical approach to the analysis of genetically-related stratigraphic elements for improved reservoir prediction. AAPG Annual Convention Abstracts (pp. 10–13).

Stevenson, C.J., Talling, P.J., Wynn, R.B., Masson, D.G., Hunt, J.E., Frenz, M., et al. (2013) The flows that left no trace: very large-volume turbidity currents that bypassed sediment through submarine channels without eroding the sea floor. *Marine and Petroleum Geology*, *41*, 186–205.

Stevenson, C.J., Jackson, C.A.L., Hodgson, D.M., Hubbard, S.M. and Eggenhuisen, J.T. (2015) Deep-water sediment bypass. *Journal of Sedimentary Research*, *85*, 1058–1081.

Symons, W.O., Sumner, E.J., Talling, P.J., Cartigny, M.J. and Clare, M.A. (2016) Large-scale sediment waves and scours on the modern

seafloor and their implications for the prevalence of supercritical flows. *Marine Geology*, *371*, 130–148.

Walker, R.G. (1975) Generalized facies models for resedimented conglomerates of turbidite association. *Geological Society of America Bulletin*, *86*, 737–748.

Walker, R.G. (1978) Deep water sandstone facies and ancient submarine fans: models for exploration of stratigraphic traps. *American Association of Petroleum Geologists Bulletin*, *62*, 932–966.

Winn, R.D. and Dott, R.H. (1977) Large-scale traction structures in deep-water fan-channel conglomerates in southern Chile. *Geology*, *5*, 41–44.

Winn, R.D. and Dott, R.H. (1979) Deep-water fan-channel conglomerates of Late Cretaceous age, southern Chile. *Sedimentology*, *26*, 203–228.

Wynn, R.B., Masson, D.G., Stow, D.A. and Weaver, P.P. (2000) Turbidity current sediment waves on the submarine slopes of the western Canary Islands. *Marine Geology*, *163*, 185–198.

Wynn, B., Piper, D.J.W. and Gee, M.J.R. (2002) Generation and migration of coarse-grained sediment waves in turbidity current channels and channel–lobe transition zones. *Marine Geology*, *192*, 59–78.

Zhong, G., Cartigny, M.J., Kuang, Z. and Wang, L. (2015) Cyclic steps along the South Taiwan Shoal and West Penghu submarine canyons on the northeastern continental slope of the South China Sea. *Geological Society of America Bulletin*, *127*, 804–824.

How to cite this article: McArthur A, Kane I, Bozetti G, Hansen L, Kneller BC. Supercritical flows overspilling from bypass-dominated submarine channels and the development of overbank bedforms. *Depositional Rec*. 2020;6:21–40. https://doi.org/10.1002/dep2.78